BIOCHEMISTRY
including biophysical chemistry & molecular biology

Article

pubs.acs.org/biochemistry

The *E. coli* Monothiol Glutaredoxin GrxD Forms Homodimeric and Heterodimeric FeS Cluster Containing Complexes

N. Yeung,[†] B. Gold,[†] N. L. Liu,[†] R. Prathapam,[†] H. J. Sterling,[‡] E. R. Willams,[‡] and G. Butland*[,†]

[†]Life Sciences Division, Lawrence Berkeley National Laboratory, Berkeley, California 94720, United States

[‡]Department of Chemistry, University of California, Berkeley, Berkeley, California 94720, United States

Supporting Information

ABSTRACT: Monothiol glutaredoxins (mono-Grx) represent a highly evolutionarily conserved class of proteins present in organisms ranging from prokaryotes to humans. Mono-Grxs have been implicated in iron sulfur (FeS) cluster biosynthesis as potential scaffold proteins and in iron homeostasis via an FeS-containing complex with Fra2p (homologue of *E. coli* BolA) in yeast and are linked to signal transduction in mammalian systems. However, the function of the mono-Grx in prokaryotes and the nature of an interaction with BolA-like proteins have not been established. Recent genome-wide screens for *E. coli* genetic interactions reported the synthetic lethality (combination of mutations leading to cell death; mutation of only one of these genes does not) of a *grxD* mutation when combined with strains defective in FeS cluster biosynthesis (*isc* operon) functions [Butland, G., et al. (2008) *Nature Methods* 5, 789−795]. These data connected the only *E. coli* mono-Grx, GrxD to a potential role in FeS cluster biosynthesis. We investigated GrxD to uncover the molecular basis of this synthetic lethality and observed that GrxD can form FeS-bound homodimeric and BolA containing heterodimeric complexes. These complexes display substantially different spectroscopic and functional properties, including the ability to act as scaffold proteins for intact FeS cluster transfer to the model [2Fe-2S] acceptor protein *E. coli* apo-ferredoxin (Fdx), with the homodimer being significantly more efficient. In this work, we functionally dissect the potential cellular roles of GrxD as a component of both homodimeric and heterodimeric complexes to ultimately uncover if either of these complexes performs functions linked to FeS cluster biosynthesis.

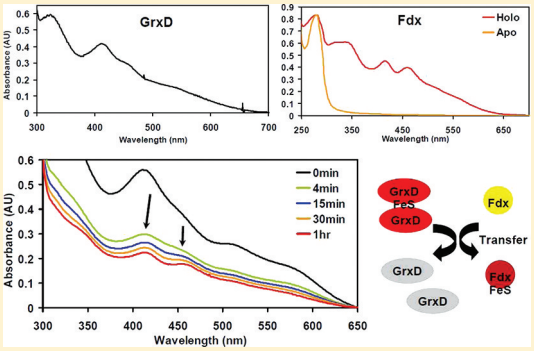

Glutaredoxins are redox proteins present in both prokaryotes and eukaryotes. CGFS-type monothiol glutaredoxins (mono-Grx) have sequence homology to classical dithiol glutaredoxins but possess a CGFS active site sequence in place of the CXXC motif present in their dithiol namesakes.[1] Detailed investigation has now revealed that mono-Grxs, while structurally similar to dithiol glutaredoxin proteins, do not function biochemically as glutaredoxins in redox chemistry.[1] Instead, studies of eukaryotic systems have connected mono-Grxs to potential roles in iron−sulfur (FeS) cluster biosynthesis, iron homeostasis, and signal transduction.[2−5]

The cellular role of monothiol glutaredoxins has been most intensely studied in *S. cerevisiae*, which encodes three CGFS-type mono-Grx homologues: Grx3p, Grx4p, and Grx5p.[1] Grx5p, which is located in the mitochondrion, is proposed to directly participate with the mitochondrial FeS cluster biosynthesis system, possibly acting to accept and/or transfer an intact FeS cluster to FeS apo-proteins.[6] Grx3p and Grx4p (herein, Grx3/4p) are cytoplasmic and display partial functional redundancy. Grx3/4p have been linked to iron regulation in *S. cerevisiae* by binding and influencing translocation of the transcriptional activator Aft1, which regulates iron uptake.[7,8] It should be noted that Grx3/4p contains an additional thioredoxin-like (Trx) domain upstream of the Grx domain that is found in all mono-Grx proteins.[1,9] However, despite these differences, recent biochemical characterization of nine monothiol glutaredoxins from a range of species, including *E. coli*, *S. cerevisiae* (Grx3/4/5p), *A. thaliana*, and human, reported that all nine proteins can exist in both a [2Fe−2S] cluster containing dimeric state and a monomeric apo protein form, suggesting a core conservation of physical properties across evolution.[10] Moreover, Grx3/4p, along with multiple prokaryotic mono-Grx proteins, were reported to be able to complement a *S. cerevisiae* Δ*grx5* mutant when localized to the mitochondrion, further outlining this functional flexibility.[11]

Global tandem affinity purification screens for protein complexes in yeast identified Grx3/4p as copurifying with two proteins of unknown function, Fra1p and Fra2p.[12,13] More detailed biochemical analysis of the complexes formed by Grx3/4p has demonstrated that both proteins can form a [2Fe−2S] containing homodimer or alternatively form a Grx3/4p-Fra2p [2Fe−2S] containing heterodimer *in vitro*.[14,15] The identification of Grx3/4p in multiple complexes with significantly different spectroscopic properties has prompted

Received: June 8, 2011
Revised: August 16, 2011
Published: September 7, 2011

speculation of multiple cellular roles in yeast, including iron regulation and iron chaperoning.[16] Conversely, very little is known regarding the function of monothiol glutaredoxins in prokaryotes. Limited functional characterization of *E. coli* GrxD[17,18] has suggested a role in cellular iron metabolism, due to increased levels of GrxD under iron limitation stress. The X-ray crystal structure of the dimeric [2Fe−2S] containing *E. coli* holo-GrxD was recently determined, with the cluster located at the dimer interface, bridging the two protomers, and coordinated by an active site cysteine (Cys-30) and non-covalently bound glutathione from each protomer.[19]

In *E. coli*, the process of FeS cluster biosynthesis is enabled by both the Isc (iron−sulfur cluster) and Suf (sulfur utilization factor) systems with the Isc system being the dominant housekeeping system and the Suf system being expressed under conditions of oxidative stress or iron limitation.[20−22] Inactivation of both the Isc and Suf systems was reported to result in synthetic lethality[21,22] and has been utilized as a "gold standard" in proof-of-principle experiments to develop a high-throughput genetic interaction screening approach in *E. coli*.[23] We previously identified the synthetic lethality of a *grxD* mutant when combined with mutations in the *isc* operon in *E. coli*.[23] These results linked *E. coli grxD* to FeS cluster biosynthesis for the first time and suggested that GrxD may function as a component of the Suf FeS cluster biosynthesis system, mutants of which display strong synthetic lethality with *isc* mutants.[21] Interestingly, while not previously observed in prokaryotes, mono-Grxs from plant chloroplasts have been suggested to function with the Suf-type chloroplast FeS cluster biosynthesis machinery, possibly acting as FeS scaffold proteins.[24] The functional picture of GrxD may be more complex, however, as affinity purification protein−protein interaction data and multiple bioinformatics approaches have linked GrxD to BolA, the bacterial ortholog of *S. cerevisiae* Fra2p.[25,26] BolA is poorly characterized but has been implicated in influencing cell morphology, particularly under stress conditions, and has been suggested to function as a transcription factor from the *in silico* prediction of a DNA binding domain.[27−30] The evolutionary conservation of the interaction of mono-Grxs and BolA orthologs prompted us to investigate the nature of the GrxD-BolA complex in *E. coli* and potential links to FeS cluster biosynthesis. Here we present data which identifies GrxD as forming FeS cluster containing complexes as both a homodimer and a heterodimer with BolA. We further show that these complexes display appreciably different physical properties. Moreover, although both protein complexes are capable of transferring their FeS clusters to apo-ferredoxin (Fdx) *in vitro*, the GrxD homodimer is significantly more proficient. These observations suggest that GrxD may perform multiple functional roles, providing impetus for determining the functional basis of the observed synthetic lethality between the *E. coli* Isc system and *grxD*.

EXPERIMENTAL PROCEDURES

UV−vis Spectroscopy. Aerobic UV−vis spectra and OD measurements were collected on a SpectraMax Plus384 spectrophotometer (Molecular Devices). Anaerobic spectra were collected on an Agilent HP 8453 spectrophotometer in an anaerobic chamber (Coy Laboratory Products), equipped with a Peltier temperature controller/stirring module. For kinetic measurements, spectra were collected every 5 or 20 s using the kinetics software package.

Analytical Gel Filtration. Analytical gel filtration was performed on a Superdex 75 PC 3.2/30 column connected to an Ettan LC system (GE Healthcare). The column was equilibrated with Gel Filtration Buffer (50 mM Tris-HCl pH 8.0, 150 mM KCl, 2 mM DTT (dithiothreitol), 1.5 mM glutathione) unless otherwise specified. Air-sensitive samples (i.e., reconstituted FeS cluster containing proteins) were taken out of the anaerobic chamber in gastight syringes and loaded immediately onto the column. Calibration was performed with the Low Molecular Weight Gel Filtration Calibration Kit (GE Healthcare). Apparent molecular weights (MW) are given as an average ± standard deviation of three or more runs.

Native Mass Spectrometry. Native electrospray ionization (ESI) mass spectrometry (MS) was performed at the University of California, Berkeley. All proteins were degassed prior to introduction into an anaerobic chamber and exchanged into 200 mM ammonium bicarbonate pH 8 containing 2 mM DTT via centrifugal concentrators (4 MWCO, Millipore). For the reconstituted GrxD homodimer and GrxD-BolA heterodimer, 1.5 mM glutathione was added to the buffer. The samples were taken out of the anaerobic chamber and frozen in liquid nitrogen. Protein samples were defrosted and diluted to ∼100−200 μM with degassed buffer immediately before MS analysis with a quadrupole time-of-flight mass spectrometer equipped with a Z-spray ion source (Q-TOF Premier, Waters). Expected MWs are calculated from the protein amino acid sequence (taking into account the presence or absence of a 6xHis tag). The expected MWs of the holo forms do not include MW contributions from the FeS clusters.

Circular Dichroism (CD). CD spectra (40 μM protein) were collected on a Jasco J-815 spectropolarimeter equipped with a Peltier temperature controller and stirring module. Apo protein spectra were collected aerobically. Reconstituted proteins were prepared in an anaerobic chamber and analyzed in sealed cuvettes. CD spectra were recorded with stirring under the following conditions: temperature = 25 °C; DIT = 2 s; bandwidth = 1 nm; accumulations = 3; data pitch = 0.1 nm, and scan speed = 50 nm/min.

CD Competition Assay: Incubation of Reconstituted GrxD with BolA. Reconstituted GrxD (150 μM, *vide infra*) was prepared in an anaerobic chamber in Reconstitution Buffer (100 mM Tris-HCl pH 8.0, 100 mM NaCl, 5 mM DTT, 1.5 mM glutathione), placed in a sealed cuvette, and brought out of the anaerobic chamber. Increasing equivalents of BolA (degassed, in Reconstitution Buffer) were added to the GrxD solution via a gastight syringe and allowed to stir for 5 min before spectra acquisition. CD spectra were recorded with conditions identical to those above except for scan speed = 100 nm/min.

Sequential Peptide Affinity (SPA) Purification of GrxD and BolA Protein Complexes. *E. coli* strains containing chromosomal *grxD* and *bolA* genes which have been modified to encode C-terminal affinity tagged alleles (referred to as *grxD-SPA* and *bolA-SPA*) were constructed previously (ref 31, Table S1). Strains bearing either *grxD-SPA* or *bolA-SPA* alleles were cultured in 5 L of Terrific Broth (TB) medium and purified as previously described.[31] Affinity purified eluates were then evaluated by SDS-PAGE and proteins visualized by silver staining. Bands were excised from the gel and subjected to in-gel digestion with trypsin followed by LC MALDI MS/MS analysis utilizing an AB 4800 TOF/TOF mass spectrometer (AB Sciex). In addition, specific samples of the purified eluate were in-solution digested and analyzed directly by LC ESI MS/

MS using a LTQ mass spectrometer (Thermo Fisher). MS experiments were performed at the University of California, San Francisco, Sandler-Moore Mass Spectrometry Core Facility.

Bacterial Strains and Plasmids Used. Plasmid vectors expressing N-terminal tagged *E. coli* 6xHis-GrxD (pET6HGrxD) and 6xHis-BolA (pET6HBolA) were created by independently amplifying the *grxD* and *bolA* genes from *E. coli* BW25113 genomic DNA by PCR and subsequent cloning of the PCR product into a pET28(b) vector (Novagen, Table S1) using NdeI and *Bam*HI restriction sites incorporated into the oligonucleotide primers. Both plasmid constructs were freshly transformed into *E. coli* BL21(DE3) prior to use. For GrxD expression, the pET6HGrxD plasmid was cotransformed with pRKISC (Table S1), which was previously observed to dramatically increase the levels of cellular FeS protein production.[32] Plasmid vectors pQE30-His-iscS and pQE30-His-fdx (obtained from Prof. Yasuhiro Takahashi, Saitama University, Japan; Table S1) were used for the expression of N-terminal 6xHis-tagged *E. coli* IscS (*iscS*) and N-terminal 6xHis-tagged *E. coli* ferredoxin (*fdx*), respectively, and the proteins were produced as previously described,[33] with the exception that pQE30-His-iscS was not cotransformed with pRKISC. A plasmid containing *grxD* under the control of an arabinose inducible promoter, pBADGrxD, was constructed by PCR amplification of *grxD* from genomic DNA and subsequent cloning of the PCR product into pBAD24 using *Eco*RI and *Hin*dIII restriction sites incorporated into oligonucleotide primers (ref 34, Table S1). Clones were selected on LB plates containing 100 μg/mL ampicillin. Plasmid DNA was isolated and positive clones were confirmed by restriction digestion. All plasmid constructs were confirmed by DNA sequencing prior to use (Elim Biopharm). All single gene mutants of *E. coli* BW25113 (i.e., *nfuA*, *grxD*, *bolA*, *yrbA*, *sufA*, *sufB*, and *sufC*) were taken from the KEIO single gene deletion collection.[35]

Protein Expression and Purification. *E. coli* cells freshly transformed with expression plasmids were grown with shaking in 1 L of TB medium at 37 °C supplemented with the appropriate antibiotics at the following concentrations: 50 μg/mL kanamycin, 12.5 μg/mL tetracycline, and 100 μg/mL ampicillin (Table S1). The cells were induced with 1 mM IPTG (isopropyl-β-D-thiogalactoside) at an OD_{600} ~0.8−1, collected by centrifugation 4 h after induction, and resuspended in Binding Buffer (20 mM Tris-HCl pH 7.9, 20 mM imidazole, 0.5 M NaCl, 10% glycerol) containing 800 μL of Complete Protease Inhibitor Cocktail (Roche). Cell free extract was prepared by sonication and loaded onto His Trap HP columns (GE Healthcare) equilibrated with Binding Buffer. The columns were washed with Wash Buffer (20 mM Tris-HCl pH 7.9, 45 mM imidazole, 0.5 M NaCl, 10% glycerol) and protein eluted with Elution Buffer (20 mM Tris-HCl pH 7.9, 0.5 M imidazole, 0.5 M NaCl, 10% glycerol). Elution fractions were examined by SDS-PAGE, and peak fractions were pooled, concentrated, and loaded onto a preparatory gel filtration column (Superdex 75 HiLoad 16/60, GE Healthcare) at 4 °C, operated with a flow rate of 0.8 mL/min on an AKTA FPLC system (GE Healthcare). The column was equilibrated with Gel Filtration Buffer (without glutathione) for GrxD, IscS, and Fdx. Column equilibration was performed instead with 20 mM Tris-HCl pH 7.9 containing 50 mM NaCl, 2 mM DTT and 10% glycerol for BolA. Peak fractions were analyzed by SDS-PAGE, and the purest fractions were pooled, concentrated, and frozen. Protein determination was performed using a BCA (Bicinchoninic Acid) assay (Pierce).

Hypersensitivity Assay of an *E. coli grxD* Mutant to Iron Depletion. LB agar plates were supplemented with 100 μg/mL ampicillin and 250 μM 2′,2-dipyridyl (Fluka) as required. The strains were inoculated into 200 μL LB liquid medium in 96-well plates and grown in a shaking incubator overnight at 37 °C. Kanamycin (25 μg/mL) was added to the mutant strain growths only. Mutant strains containing pBADGrxD were grown in medium containing an additional 100 μg/mL ampicillin. After overnight growth, the OD_{600} of each strain was taken and normalized using LB liquid medium so that each strain had an equal number of cells to be plated. Serial dilutions (1:10) of each strain were made using sterile water, and 10 μL of each of these dilutions was spotted sequentially onto LB agar plates with and without ampicillin and/or 2′,2-dipyridyl. The plates were incubated at 32 °C overnight, and the growth was assessed for sensitivity to iron depletion.

Preparation of Apo-GrxD Protein. Apo-GrxD was obtained as previously reported.[10]

Preparation of Apo-Fdx Protein. Apo-Fdx was prepared as previously reported[36] and desalted with a PD-10 column.

Cleavage of the 6xHis Affinity Tag. The affinity tag on apo-GrxD was cleaved by incubation of 150 μg of protein with 20 U of thrombin (Calbiochem, human plasma, high activity) in 20 mM Tris-HCl pH 8.4 containing 150 mM NaCl and 2.5 mM $CaCl_2$ for 2 h at room temperature. Sequential His Trap HP and HiTrap Benzamidine FF columns (GE Healthcare) were used to separate uncleaved protein and thrombin, respectively, from cleaved apo-GrxD, and both separations were confirmed by SDS-PAGE.

Reconstitution of the FeS Cluster in Fdx. Apo-Fdx (300 μM) was incubated in an anaerobic chamber at 28 °C with 0.014 equiv of IscS and 10 equiv of L-cysteine in Reconstitution Buffer without glutathione. All components were degassed before introduction into an anaerobic chamber. Reconstitution reactions were set up to include all components except $FeCl_3$ and incubated with constant stirring for 20 min. Reconstitution was initiated by slow addition of 8 equiv of $FeCl_3$ (hexahydrate, Sigma-Aldrich). The protein mixture was allowed to mix for a further ~10 min before desalting with a PD-10 column equilibrated with Reconstitution Buffer.

Reconstitution of the FeS Cluster in GrxD. Apo-GrxD or affinity tag cleaved apo-GrxD was reconstituted under conditions identical to apo-Fdx with the following exceptions. Reconstitution was performed in the presence of 10 equiv glutathione. Either 6 equiv of $FeCl_3$ was added to more concentrated protein samples (>150 μM) or 8 equiv of $FeCl_3$ was added to 150 μM protein. The reaction was allowed to run for ~2 min before desalting as above.

Formation of a GrxD-BolA Heterodimer. His tag cleaved apo-GrxD (250 μM) and BolA (125 μM) were incubated for 1 h in an anaerobic chamber at 28 °C in Reconstitution Buffer without glutathione.

Reconstitution of the FeS Cluster in a GrxD-BolA Heterodimer. Reconstitution was performed under apo-GrxD reconstitution conditions with 250 μM affinity tag cleaved apo-GrxD and 125 μM BolA. The reaction was stirred for 1.5 h after addition of 6 equiv of $FeCl_3$ with respect to cleaved apo-GrxD. Reconstituted GrxD homodimer (6xHis cleaved) and GrxD-BolA heterodimer were separated on a His Trap HP column equilibrated with Binding Buffer and then washed with Wash Buffer (2 mM DTT and 1.5 mM glutathione were added to both buffers). The heterodimer fraction was

eluted with Elution Buffer containing 2 mM DTT and 1.5 mM glutathione and desalted on a PD-10 column equilibrated with Reconstitution Buffer.

FeS Cluster Transfer to Apo-Fdx. In an anaerobic chamber, 85 μM of either reconstituted GrxD homodimer or GrxD-BolA heterodimer (diluted with Reconstitution Buffer) was placed in a cuvette. As uncleaved and cleaved apo and reconstituted holo-GrxD have the same physical properties (by CD, Figure S4), 6xHis-apo-GrxD was used in the homodimer reconstitution reactions to avoid the unnecessary step of cleaving the 6xHis tag. UV−vis spectra acquisition was started prior to the addition of 0.214 equiv of EDTA to the protein. EDTA chelates adventitious iron ions released in solution by FeS cluster degradation (if any) to ensure that any transfer detected is from intact FeS cluster transfer and not cluster destruction and re-formation. Next, 1 equiv of of apo-Fdx was added to the protein/EDTA solution. An aliquot of the transfer reaction was evaluated by analytical gel filtration after ~2 min (control, earliest time point that could be collected) and 1 h of incubation. To estimate the fraction of FeS cluster transferred to apo-Fdx, the 414 nm intensity of the homodimer or heterodimer (analytical gel filtration profile) after 1 h of incubation was compared to an aliquot of the respective protein at an identical concentration before transfer. The protein used for a set of transfer reactions (i.e., before transfer, 2 min, and 1 h) were derived from the same reconstitution reaction to ensure that transfer reactions from different time points were comparable. Alternatively, 45 μM of reconstituted protein with 1 equiv of apo-Fdx was incubated as above, with bathophenanthroline (3 equiv, disulfonic acid disodium trihydrate, Sigma-Aldrich) as the chelator to confirm the results observed with EDTA.

RESULTS

The *grxD* Mutant Is Hypersensitve to Iron Depletion. Mutants of the Suf system have previously been reported to be hypersensitive to the depletion of iron in the growth medium upon addition of the free iron chelator 2′,2-dipyridyl.[22] To evaluate the potential link between GrxD and members of the Suf system, we investigated the sensitivity of a *grxD* mutant to iron depletion and correlated this sensitivity to that of three *suf* operon mutants (*sufA*, *sufB*, and *sufC*) and a mutant in the alternative A-type scaffold, *nfuA*, that also displays hypersensitivity.[37] The *bolA* mutant and the *bolA* homologue, *yrbA*, were also tested for sensitivity to iron depletion. The *sufB*, *sufC*, and *nfuA* mutants were extremely sensitive to the depletion of iron, with *sufA* mutants appearing only slightly sensitive (Figure 1, left panel). These results are consistent with previous work.[22,37] The *grxD* mutant also displayed high sensitivity to iron depletion, although some growth was observed throughout the dilution series and the sensitivity judged to be slightly less severe than *sufB*, *sufC*, or *nfuA* mutants. No sensitivity was observed for the *bolA* and *yrbA* mutants, which behaved like the control (*ybaS* mutant). This experiment was repeated after transformation of the arabinose inducible pBADGrxD plasmid (Figure 1, right panel) into the above strains. When tested for sensitivity, these strains behaved as strains without the additional plasmid, except in the case of *grxD* which displayed stronger growth, consistent with complementation.

Sequential Peptide Affinity (SPA) Purification Reveals That GrxD and BolA Physically Interact with Each Other. The genetic and phenotypic links between *grxD* and *suf* operon mutants prompted us to re-examine existing physical interaction data for GrxD to determine if any of the proteins copurifying with GrxD could give clues to its function in *E. coli*. Analysis of data reported from a previous global study of protein−protein interactions in *E. coli* revealed that GrxD copurified with SPA-tagged BolA, but the reciprocal copurification (i.e., BolA copurifying with SPA-tagged GrxD) was not observed.[31] We revisited the SPA purification and mass spectrometry analysis of GrxD and BolA using larger volumes of material in an attempt to show the reciprocal association of these two proteins *in vivo*. The SDS-PAGE analysis of BolA- and GrxD-SPA purifications is shown in Figure 2. Mass spectrometry confirmed the reciprocal copurification of GrxD with BolA. However, whereas GrxD and BolA are the two most abundant proteins in the BolA-SPA purified eluate, the GrxD-SPA eluate repeatedly contains a relatively small amount of BolA by LC MALDI MS/MS mass spectrometry of silver stained gel bands or direct analysis by LC ESI MS/MS mass spectrometry (data not shown). These data indicate that, in addition to the previously reported homodimeric [2Fe−2S] containing complex,[10,19] *E. coli* GrxD can form a heteromeric complex with BolA. Additional copurifying proteins (i.e., DnaN, RfaD) as identified by MALDI-MS are commonly found in SPA purifications and not likely relevant to *E. coli* FeS cluster biosynthesis.[31] Despite using larger culture volumes (5 L), several bands in both the BolA-SPA and GrxD-SPA purifications could not be identified by MALDI-MS due to insufficient yield.

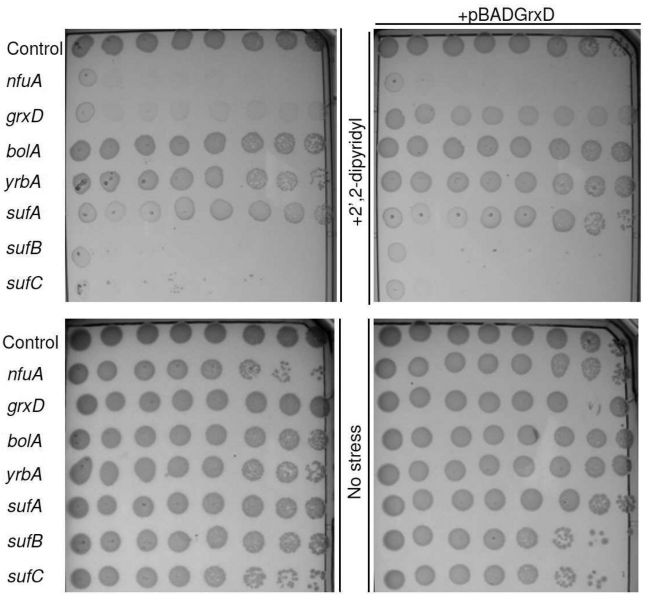

Figure 1. Hypersensitivity of a *grxD* mutant to Fe depletion. *E. coli* strains bearing the indicated mutations were serially 10-fold diluted in LB medium and spotted in equal volumes sequentially across the plate from left to right. Left panel: strains containing no plasmid were spotted onto LB medium supplemented with 250 μM 2′,2-dipyridyl (top) and LB medium without supplement as a control (bottom). Right panel: mutant strains transformed with pBADGrxD were spotted onto LB medium supplemented with 250 μM 2′,2-dipyridyl (top) and LB medium without supplement as a control (bottom).

Purification and Characterization of *E. coli* GrxD. To characterize the complexes formed by GrxD in more detail, N-terminal 6xHis tagged GrxD (6xHis-GrxD) was constructed, grown, purified and evaluated by analytical gel filtration and UV−vis spectroscopy. Herein, 6xHis-GrxD will be called GrxD

dx.doi.org/10.1021/bi2008883 | *Biochemistry* 2011, 50, 8957−8969

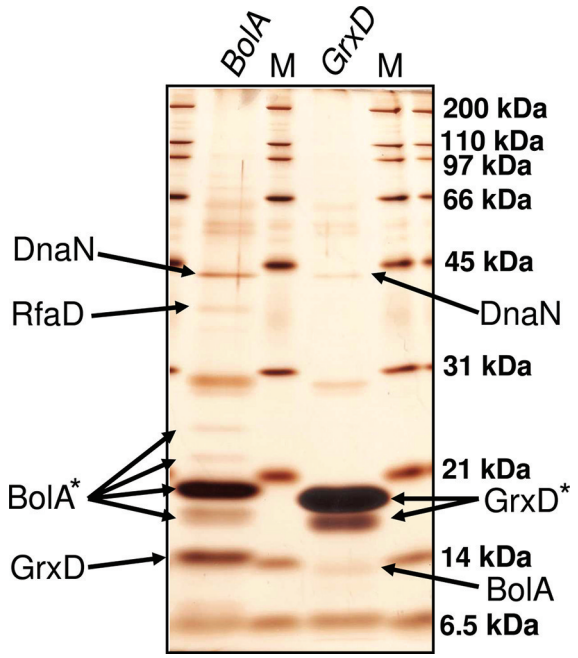

Figure 2. Silver stained SDS-PAGE analysis of GrxD-SPA and BolA-SPA purified protein complexes. Proteins present in gel bands that have been identified by LC MALDI MS/MS are indicated by arrows. SPA-tagged proteins are denoted by an asterisk.

unless otherwise noted. The UV−vis spectrum of as prepared GrxD shows peaks at 414 and 456 nm (Figure 3A). Analytical gel filtration of purified GrxD (1 mM) resulted in two partially resolved peaks in the 280 nm profile migrating at apparent MWs of 37.6 ± 2.1 and 20.2 ± 2.9 kDa and a single peak in the 414 nm profile, correlating exactly with the ∼38 kDa peak in the 280 nm profile (Figure 3B and Table 1). The association of the 414 nm absorption with the higher molecular weight peak is consistent with GrxD binding a [2Fe−2S] cluster in the dimeric form and is in good agreement with previous studies of GrxD from other species and recent structural data.[10,19] It should be noted that the mass values reported above, obtained after repeated column calibration, were significantly larger than the sequence predicted MW of GrxD at 15 042 Da (Table 1). To confirm the true size of the expressed protein, we analyzed intact GrxD by electrospray mass spectrometry (Figure S1 and Table 1). These MS data revealed charge state distributions corresponding mainly to monomeric GrxD without the leading methionine and a smaller contribution from monomeric GrxD with the leading methionine, matching its expected molecular weight. Charge state distributions corresponding to GrxD complexes with bound FeS clusters were not observed in this study, suggesting that the FeS clusters in these complexes are labile and prone to degradation during the ionization process. Repeated observations indicated that GrxD was isolated ("as prepared") as a mixture of the apo monomeric and holo dimeric forms, which displayed batch-to-batch variation in ratio. Therefore, to verify the above observations and to ensure that

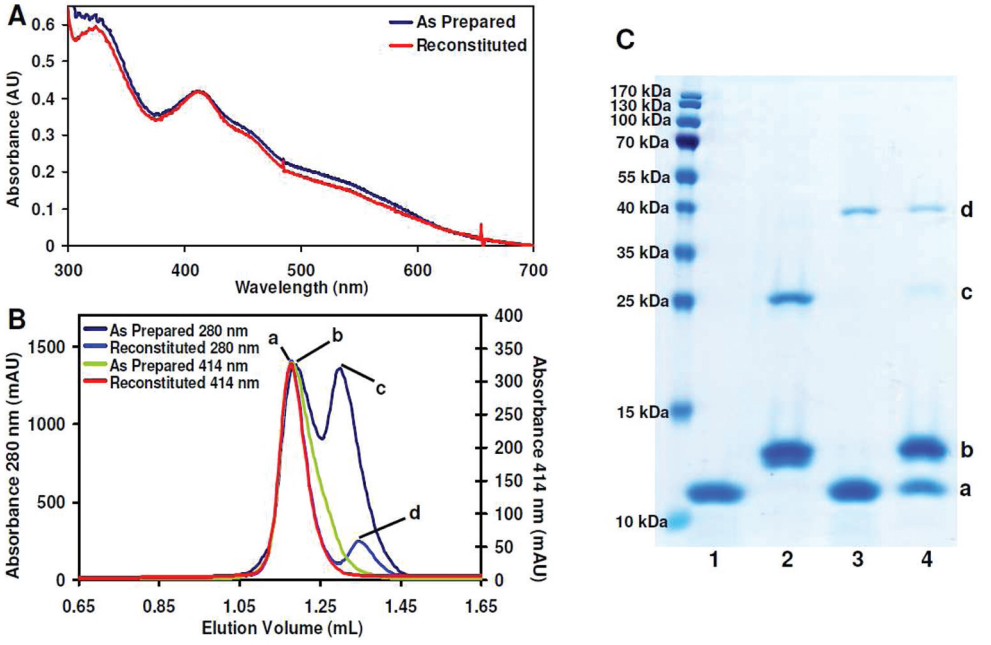

Figure 3. (A) UV−vis spectroscopy of as prepared and reconstituted GrxD. UV−vis spectra have been baseline corrected and normalized (i.e., for qualitative purposes, spectra have been plotted using an identical absorbance range). (B) Analytical gel filtration elution profiles of as prepared and reconstituted GrxD. Elution profiles were recorded for 280 nm (protein profile) and 414 nm (FeS cluster profile) with a flow rate of 0.05 mL/min on an Ettan LC (GE Healthcare), baseline corrected, and normalized. Average apparent MW ± standard deviation of (a) reconstituted GrxD homodimer = 39.4 ± 1.3 kDa; (b) as prepared GrxD homodimer = 37.6 ± 2.1 kDa; (c) as prepared GrxD monomer = 20.2 ± 2.9 kDa; and (d) reconstituted GrxD monomer = 17.3 kDa ± 1.9 kDa. Expected MW: GrxD homodimer = 30 084 Da; GrxD monomer = 15 042 Da. (C) SDS-PAGE analysis of the purity and composition of a GrxD homodimer and GrxD-BolA heterodimer. Purified sample of affinity tag cleaved apo-GrxD (lane 1), 6xHis-BolA (lane 2), reconstituted cleaved GrxD homodimer (lane 3), and high imidazole elution fraction after His Trap and PD-10 column purification of GrxD-BolA heterodimer (lane 4). Identity of bands: (a) cleaved apo-GrxD, (b) BolA, (c) BolA (dimer), and (d) IscS (used in the reconstitution reaction). Expected MW: cleaved apo-GrxD = 13 160 Da; BolA = 14 157 Da; IscS ∼47 kDa. Expected MWs are calculated from the amino acid sequence (taking into account the presence or absence of a 6xHis tag).

dx.doi.org/10.1021/bi2008883 | *Biochemistry* 2011, 50, 8957−8969

Table 1. Molecular Weight Analysis of GrxD and BolA Proteins and Complexes by Various Methods

protein	expected[a] (Da)	analytical gel filtration (av ± std dev) (kDa)	mass spectrometry (Da) (MS)[b]	notes
BolA	14 157	14.6 ± 0.2	14 024 ± 3	analytical gel fitration: analysis of 10 μM protein
apo-GrxD	15 042	18.2 ± 0.4		
cleaved apo-GrxD	13 160	17.8 ± 0.4		6xHis tag is cleaved
as prepared GrxD				
monomer (apo)	15 042	20.2 ± 2.9	14 907 ± 7	
homodimer (holo)	30 084	37.6 ± 2.1	29 823 ± 1	
reconstituted GrxD				
monomer (apo)	15 042	17.3 ± 1.9	14 911 ± 1	
homodimer (holo)	30 084	39.4 ± 1.3	29 822 ± 1	
GrxD-BolA heterodimer	27 317	30.6 ± 0.3	27 182 ± 3	6xHis tag is cleaved on apo-GrxD
		28.4 ± 1.4[c]		

[a]Calculated from the amino acid sequence taking into account the presence or absence of a 6xHis tag; the expected molecular weight of the holo form does not include the molecular weight due to the FeS cluster. [b]Minus leading methionine; likely due to proteolysis. [c]Apo form, without FeS cluster.

the protein is consistently in one of the above forms for downstream analysis, we removed the FeS cluster from as prepared GrxD in order to reconstitute an FeS cluster into the resulting apoprotein (see Experimental Procedures). Analytical gel filtration of apo-GrxD resulted in a single peak in the 280 nm profile migrating at 18.2 ± 0.4 kDa (Figure S2 and Table 1), which is similar in size to as prepared monomeric GrxD by analytical gel filtration (within one standard deviation, Table 1). The generation of the apo form of GrxD resulted in a loss of the FeS cluster and concomitant transition to the monomeric form.

Despite the accurate expected mass values obtained by mass spectrometry, we could not rule out that the aberrant size migration of apo- and holo-GrxD by analytical gel filtration was due to the presence of the 6xHis tag. We therefore incubated apo-GrxD with thrombin protease to cleave the affinity tag. Cleavage was assessed by SDS-PAGE to be >90% effective (Figure S3A) as judged by distinct migration of His tag cleaved and uncleaved GrxD (Figure S3B). The CD spectra of His tag cleaved and uncleaved GrxD in the reconstituted (*vide infra*) and apo forms were found to be identical (Figure S4), indicating that the presence of the 6xHis tag does not affect protein structure or its migration as assayed by analytical gel filtration or SDS-PAGE.

Reconstitution of apo-GrxD with an FeS cluster was achieved with $FeCl_3$, L-cysteine, glutathione, and the cysteine desulfurase IscS.[37] The UV−vis spectrum of reconstituted GrxD (Figure 3A) is comparable to the as prepared form with absorbances at 414 and 456 nm, suggesting that *in vitro* FeS cluster reconstitution of the apoprotein results in a holoprotein very similar to as prepared GrxD. Reconstitution could not be achieved without glutathione, which is in agreement with previous work and recent GrxD structural studies where glutathione was found to be an essential FeS cluster ligand.[10,19] Reconstituted GrxD displays a main peak in the 280 and 414 nm elution profiles at 39.4 ± 1.3 kDa (Figure 3B and Table 1), which we attribute to homodimeric FeS cluster containing GrxD. A minor peak in the 280 nm profile of reconstituted GrxD at 17.3 ± 1.9 kDa likely represents the unreconstituted apo-GrxD monomer (Table 1). Based on this analysis, ∼80−90% reconstitution of an FeS cluster into apo-GrxD is typically achieved.

Electrospray mass spectrometry (Figure S5 and Table 1) detected the presence of an FeS cluster free GrxD homodimer (after reconstitution). However, the main signal is that of the GrxD monomer, which was expected as the FeS cluster in GrxD is labile and susceptible to degradation with concomitant conversion of the dimer to the monomeric form. The MS data, together with UV−vis data, are consistent with that observed for as prepared GrxD, reaffirming that reconstituted GrxD has identical physical properties to as prepared GrxD. Furthermore, the above results show that although the FeS cluster in GrxD is labile, it is possible to perform IscS-dependent reconstitution to rebuild an FeS cluster into GrxD.

Purification and Characterization of *E. coli* BolA. To determine the nature of the relationship between BolA and GrxD, as identified by affinity copurification (Figure 2), affinity tagged 6xHis-BolA (BolA) was purified and analyzed by analytical gel filtration and UV−vis spectroscopy. A 160 μM sample of BolA resulted in a broad peak in the 280 nm profile corresponding to an apparent molecular weight of 22.8 ± 0.6 kDa. Affinity tagged BolA is predicted by sequence to be 14 157 Da. Therefore, similar to GrxD, BolA also migrates faster than expected. Significantly, the apparent molecular migration of BolA by analytical gel filtration is concentration-dependent (Figure S6). For instance, a much lower concentration of BolA (10 μM) gives an apparent molecular weight of 14.6 ± 0.2 kDa, which is close to the expected MW of BolA (Table 1). This concentration dependence was not detected for any of the other proteins in this study. Furthermore, BolA dimerization was apparent by SDS-PAGE (Figure 3C, lane 2), where a weaker, higher MW band can be observed at ∼26 kDa, in agreement with the expected size of a BolA dimer. Mass spectrometry of BolA is consistent with the expression and purification of a protein at 14 024 ± 3 Da (Figure S7 and Table 1). Also present are signals corresponding to a BolA dimer and tetramer. Therefore, it is possible that at higher concentrations BolA exists as dimer in solution and may change multimeric state based on concentration, consistent with gel filtration data (Figure S6).

dx.doi.org/10.1021/bi2008883 | *Biochemistry* 2011, 50, 8957−8969

Formation and Characterization of a GrxD-BolA Heterodimer Complex and *in Vitro* Reconstitution of an FeS Cluster into the GrxD-BolA Heterodimer. Sequential peptide affinity purification and mass spectrometry data have demonstrated the reciprocal copurification of GrxD with BolA (Figure 2, ref 31). To confirm this interaction and to provide enough protein for biochemical characterization, we attempted to reconstitute a GrxD-BolA complex *in vitro*. Moreover, if successful, we wanted to investigate whether the GrxD-BolA protein complex, like that of the GrxD homodimer, could form and bind an FeS cluster. To this end, we incubated untagged apo-GrxD (250 μM) with tagged BolA (125 μM) in the absence of both exogenous iron and glutathione and examined the mixture by analytical gel filtration. The 280 nm elution profile (Figure 4A, blue profile) shows a dominant peak

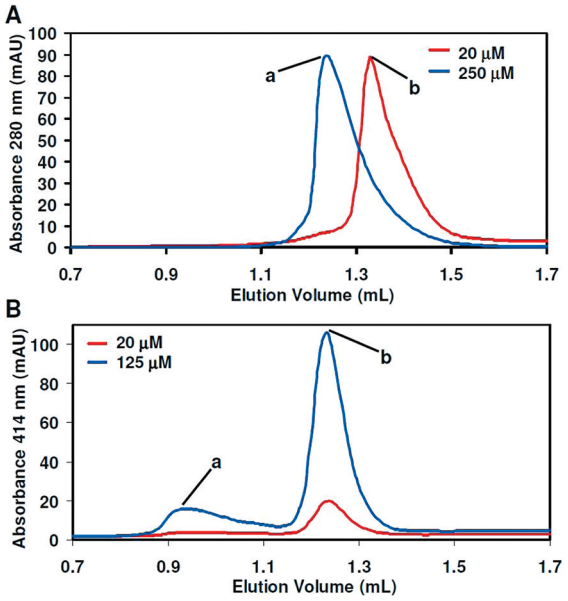

Figure 4. Analytical gel filtration of apo- and holo-GrxD-BolA heterodimer (expected MW = 27 317 Da). (A) Concentration-dependent formation of apo-GrxD-BolA. Average apparent MW: (a) 28.4 ± 1.4 kDa and (b) 19.2 ± 0.4 kDa. The profiles were normalized to the 20 μM concentration profile (i.e., for qualitative purposes, both profiles have been plotted using an identical absorbance range). (B) Concentration-independent formation of holo-GrxD-BolA. Average apparent MW: (a) 120 kDa ± 10.8 kDa (tetramer of b)) and (b) GrxD-BolA = 30.6 ± 0.3 kDa. Only the 414 nm peak is shown for clarity. All concentrations are based on apo-GrxD concentration.

with an apparent MW of 28.4 ± 1.4 kDa. Significantly, the peak at ~28 kDa is indicative of the formation of a higher MW protein complex as both the apparent molecular weights of cleaved apo-GrxD (~18 kDa, concentration independent) and BolA (~23 kDa at 160 μM) are considerably smaller. This observation shows that GrxD and BolA can indeed bind to one another to form a heterodimeric GrxD-BolA complex (expected MW = 27.3 kDa, Table 1). However, when the heterodimer complex was diluted (20 μM apo-GrxD:10 μM BolA), the ~28 kDa species is replaced by one at 19.2 ± 0.4 kDa (Figure 4A, red profile), which is most similar to cleaved apo-GrxD. The contribution from BolA is likely buried beneath the more intense and broad apo-GrxD absorbance as a 10 μM concentration of BolA has an apparent MW of ~15 kDa (Table 1). Thus, these data suggest that the heterodimeric complex formed by GrxD and BolA is unstable and dissociates at low concentrations.

To establish the FeS cluster binding ability of the GrxD-BolA heterodimer, cleaved apo-GrxD was incubated with 0.5 eq of 6xHis-BolA under the same reconstitution conditions as the GrxD homodimer, allowed to incubate for 1.5 h in an anaerobic chamber and purified by (His Trap) affinity chromatography (see Experimental Procedures). A dark brown band was observed at the top of the His Trap column which could only be eluted at a high imidazole concentration. SDS-PAGE analysis (Figure 3C, lane 4) of the dark brown solution after high imidazole elution and PD-10 column purification showed that the fraction was comprised primarily of proteins with an identical migration to cleaved apo-GrxD and 6xHis-BolA, with weak bands contributed from IscS and what is likely a 6xHis-BolA dimer. BolA alone does not appear to bind an FeS cluster as repeated attempts to reconstitute a cluster into BolA were unsuccessful (as monitored by UV−vis and analytical gel filtration; data not shown).

To determine the stoichiometry of this complex and to confirm the presence of an FeS cofactor, we subjected the heterodimeric complex (~125 μM) to analytical gel filtration. A single dominant peak in the 280 and 414 nm profiles (Figure 4B, blue profile) was observed, corresponding to a molecular weight of 30.6 ± 0.3 kDa (expected MW = 27.3 kDa, Table 1), which is ~9 kDa lighter than the apparent MW of the reconstituted GrxD homodimer (see Figure S8 for a comparison). In addition, a slight shoulder at ~14 kDa was observed in only the 280 nm profile (data not shown), likely corresponding to a small percentage of monomeric 6xHis-BolA which could not be separated from the reconstitution reaction by affinity chromatography. The presence of a single cofactor containing peak at ~31 kDa strongly suggests that reconstitution of GrxD and BolA under these conditions results in the formation of an FeS cluster containing GrxD-BolA heterodimer. In contrast to the cluster free form, dilution of holo-GrxD-BolA to 20 μM for analytical gel filtration (Figure 4B, red profile) revealed a cluster containing protein with an apparent MW of 29.8 ± 0.5 kDa, coinciding with the concentrated FeS cluster bound heterodimer (Figure 4B, blue profile). The UV−vis spectrum of holo-GrxD-BolA displayed features typical of the presence of an FeS cluster but was subtly and distinctly different from that of the GrxD homodimer (Figure S9). The main peak absorbance is slightly blue-shifted (λ_{max} = 413 nm) but broadened significantly (i.e., no distinct peak at 456 nm) in comparison to the GrxD homodimer. No features typical of an FeS cluster were present when the heterodimer was reconstituted in the absence of glutathione, indicating that a glutathione molecule may also provide an FeS ligand to GrxD when present in the heterodimer complex (data not shown). Mass spectrometry of the FeS containing heterodimer shows two dominant charge state distributions (Figure S10) corresponding to BolA and cleaved GrxD. A less dominant distribution from a protein of 27 182 ± 3 Da, corresponding to the expected MW of GrxD-BolA (Table 1) is also present. The above results show that BolA and GrxD can interact with each other to form a heterodimeric complex and that the physical properties of the GrxD-BolA heterodimer in solution (UV−vis and analytical gel filtration) differ distinctly from that of the GrxD homodimer.

To determine which of the holo complexes, the GrxD homodimer or the GrxD-BolA heterodimer, is the more thermodynamically favored form, reconstituted holo-GrxD

dx.doi.org/10.1021/bi2008883 | *Biochemistry* 2011, 50, 8957−8969

was incubated with increasing equivalents of BolA and followed by CD. The CD spectra of the holo-GrxD homodimer and holo-GrxD-BolA heterodimer complexes are very distinct from one another (Figure 5A), facilitating the observation of a possible homodimer to heterodimer conversion. Indeed, CD data (Figure 5B) of the anaerobic incubation of BolA with holo-GrxD clearly show a gradual conversion of the GrxD homodimer to the GrxD-BolA heterodimer spectrum with increasing BolA concentrations. Conversion to a predominantly heterodimeric form occurs after the addition of ~0.5 equiv of BolA with the appearance of complete conversion and little or no GrxD character after the addition of 2.0 equiv of BolA.

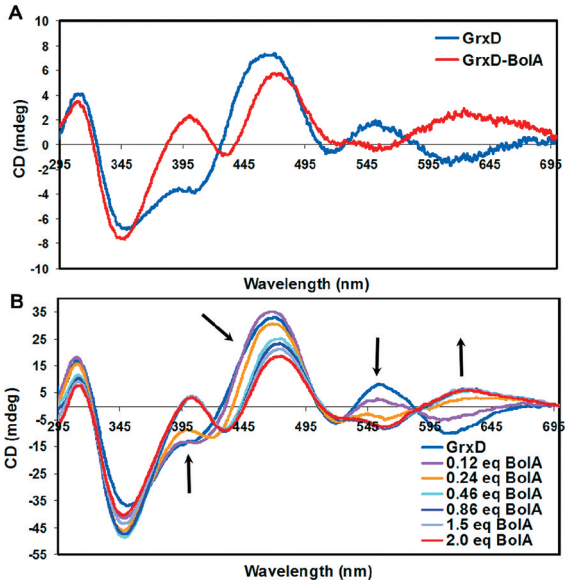

Figure 5. CD spectroscopy of GrxD homodimer conversion to GrxD-BolA heterodimer in the presence of BolA. (A) Reconstituted GrxD homodimer and GrxD-BolA heterodimer. (B) Anaerobic incubation of reconstituted GrxD (40 μM) with increasing equivalents of BolA. BolA was added with stirring and allowed to mix with GrxD for 5 min before spectra acquisition. The CD spectra shown are not dilution corrected and BolA equivalents were calculated after dilution. Arrows indicate gross changes in the CD spectrum of the FeS cluster containing species after incubation with increasing equivalents of BolA.

GrxD Homodimer Can Transfer Its FeS Cluster to Apo-Fdx. Our observation of differences in stability between the homodimer and heterodimer, both with and without FeS clusters, prompted us to test these proteins for differences in FeS cluster transfer/scaffolding ability. Reconstituted GrxD homodimer was incubated in an anaerobic chamber with 1 equiv of apo-Fdx (frequently used as a model acceptor protein capable of receiving an intact FeS cluster) and EDTA (chelating agent). The reaction was followed continuously by UV−vis spectroscopy. Significant changes to the UV−vis spectrum, such as the formation of characteristic holo-Fdx visible absorption peaks at 416 and 460 nm, can be detected in as little as 4 min. The spectrum changes entirely from GrxD character (Figure 6) to significant holo-Fdx character after 1 h. After ~2 min and 1 h of incubation, an aliquot of the transfer reaction was analyzed by analytical gel filtration (Figure 7A). The 414 nm elution profile at ~2 min (Figure 7A, blue profile) shows that the majority of the FeS cluster containing protein is of an apparent MW of 39.4 ± 1.3 kDa, corresponding to holo-GrxD dimer. However, even at ~2 min a small fraction of an FeS cluster containing 16.6 ± 0.1 kDa protein, corresponding to holo-Fdx (Figure 7A, green profile) can be seen clearly. At 1 h of incubation (Figure 7A, red profile), the majority of the FeS cluster resides in holo-Fdx. We estimate that approximately 3/4 of total FeS cluster content present in the GrxD homodimer was transferred to holo-Fdx based on the amount of FeS cluster remaining after 1 h of incubation (see Experimental Procedures). Similar transfer experiments were performed using bathophenanthroline as an alternative iron chelator to confirm the results obtained with EDTA. FeS cluster transfer was not inhibited by bathophenanthroline and the extent of transfer was similar to that in the presence of EDTA (data not shown). These results reveal that the *E. coli* GrxD homodimer is able to efficiently donate its FeS cluster to an acceptor protein such as apo-Fdx.

GrxD-BolA Heterodimer Can Transfer Its FeS Cluster to Apo-Fdx. The reconstituted GrxD-BolA heterodimer was also tested for its ability to transfer its FeS cluster to apo-Fdx. In contrast to the GrxD homodimer, distinctive holo-Fdx peaks at 416 and 460 nm were not observed with the GrxD-BolA heterodimer until ~1 h of incubation (Figure S11). Consistent with spectroscopic observations, analytical gel filtration analysis of the 414 nm profile at ~2 min (Figure 7B, blue profile) shows that the majority of the FeS cluster is contained in a 30.6 ± 0.3 kDa protein, coinciding with the GrxD-BolA heterodimer, with some retained in a protein at 120 ± 10.8 kDa, corresponding to a GrxD-BolA tetramer. After 1 h of incubation (Figure 7B, red profile), distinct holo-Fdx formation was detected although the majority of the FeS cluster still resides on the heterodimer. We estimate that less than 1/3 of total FeS cluster content was transferred from the GrxD-BolA heterodimer to holo-Fdx (vs ~3/4 from the homodimer). Substitution of EDTA with bathophenanthroline resulted in no significant changes to the extent of FeS cluster transfer, suggesting that intact cluster transfer was taking place (data not shown). Therefore, while the heterodimer shows some capacity for intact cluster transfer, this process is significantly impaired when compared to the GrxD homodimer where the majority of the FeS cluster was transferred to Fdx after 1 h.

DISCUSSION

The increased characterization of CGFS-type monothiol glutaredoxins from a range of species has linked this class of proteins to roles in both FeS cluster biosynthesis and iron homeostasis.[16,24] The vast majority of these reports however have been based on eukaryotes, with only a handful of reports characterizing bacterial mono-Grx function.[17,18] We recently linked the sole *E. coli* mono-Grx, GrxD, to FeS cluster biosynthesis in this organism by demonstrating strong synthetic lethality of a *grxD* mutant with mutations in the housekeeping FeS cluster biosynthesis (*isc*) operon.[23] Here we reconcile these results with our previous observation of GrxD copurifying with affinity purified *E. coli* BolA by demonstrating for the first time that a single domain mono-Grx such as GrxD can form both homodimeric and heterodimeric (with BolA) FeS cluster containing complexes which display distinct physical properties including the capacity for intact FeS cluster transfer to a model FeS apoprotein.[24,31,36] These data indicate that GrxD may form multiple complexes in the cell with distinct functional roles and will greatly facilitate our efforts to understand the molecular basis of *grxD/isc* synthetic lethality.

GrxD Is Absolutely Necessary under Iron Depletion Conditions and Functionally Linked to Suf. Phenotypic

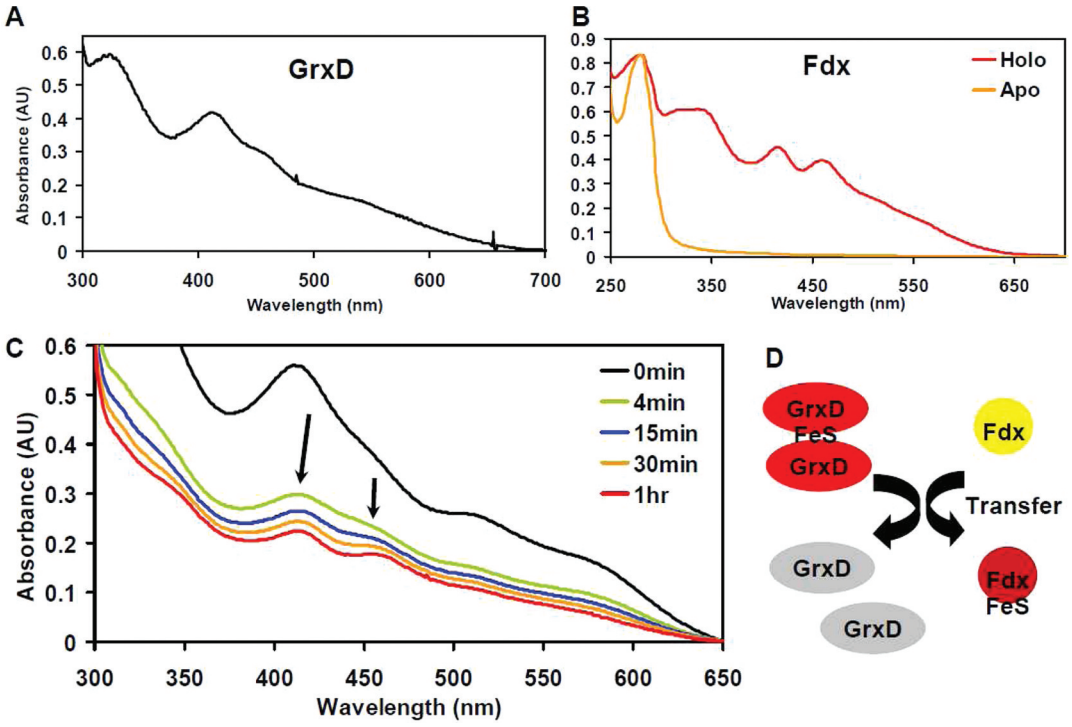

Figure 6. GrxD can act as a scaffold protein: FeS cluster donation to apo-ferredoxin (Fdx). (A) UV−vis spectrum of as prepared GrxD (mixture of holo and apo forms; only the holo form has an absorbance in the visible spectrum). (B) UV−vis spectra of apo-Fdx and holo-Fdx. (C) UV−vis spectra over time of FeS cluster transfer from reconstituted GrxD (85 μM) to 1 equiv of apo-Fdx in 0.1 M Tris-HCl pH 8.0 containing 0.1 M NaCl, 5 mM DTT, 1.5 mM glutathione and 0.214 equiv of EDTA. (D) Schematic diagram of FeS cluster transfer from holo scaffold protein (e.g., GrxD homodimer) to apo acceptor protein (e.g., apo-Fdx), resulting in the conversion of GrxD from the holo dimeric to apo monomeric form. Arrows indicate transitions in the UV−vis spectra over time. All UV−vis spectra were baseline corrected.

characterization showed that the growth of a *grxD* mutant was sensitive to iron depletion in the presence of 2′,2-dipyridyl (Figure 1). This sensitivity, taken together with the observed synthetic lethality of *grxD*/*isc* operon double mutants, further functionally links GrxD to the Suf system as *suf* operon mutants are also synthetically lethal in combination with *isc* operon mutants and sensitive to 2′,2-dipyridyl.[22] Moreover, with the exception of the *grxD* mutant, the lack of cross-complementation in mutant strains by overproduction of GrxD (Figure 1, right panel) suggests that GrxD does not facilitate an independent mechanism of resistance to iron depletion. Taking into consideration the characterization of GrxD and BolA containing complexes herein, the hypersensitivity displayed by the *grxD* mutant may be ascribed to the absence (and corresponding loss of cellular function) of monomeric apo-GrxD or the FeS cluster containing GrxD homodimer. The hypersensitivity phenotype is likely not attributed to the loss of functional GrxD-BolA heterodimer in the cell, as the *bolA* mutant is resistant to iron depletion. This observation further highlights the functional differences between GrxD and GrxD-BolA complexes and underscores the importance of interpreting phenotypic data in the context of loss of function of specific protein complexes.

GrxD and BolA Interact and Are Both Functionally Linked to FeS Cluster Biosynthesis. The demonstration of reciprocal copurification of *E. coli* GrxD and BolA (Figure 2, ref 31) represents the only experimental evidence linking GrxD and BolA in prokaryotes. In contrast, monothiol glutaredoxins have been linked to iron regulation in yeast via an FeS containing complex with Fra2p, a homologue of *E. coli* BolA.[14,15] However, yeast Grx3/4p are dual domain proteins, containing both a thioredoxin and glutaredoxin domain, while *E. coli* GrxD only contains a glutaredoxin domain. The identification of a GrxD-BolA complex in this work suggests that the GrxD-BolA interaction is mediated via the core glutaredoxin domain. Although informatics studies[25,26] show that the interaction of mono-Grxs and BolA appear to be strongly conserved across evolution, functional divergence may have taken place. This proposal is supported by work in *S. cerevisiae*, where dual-domain Grx3/4p were found to be essential to intracellular iron trafficking, whereas single domain glutaredoxins were unable to perform this function.[16,38]

Although affinity copurification data confirm that GrxD and BolA form a complex, it does not directly implicate BolA in FeS cluster biosynthesis. However, in addition to the evolutionary conservation of the GrxD-BolA interaction, selected SufE (sulfur transfer protein, member of Suf FeS cluster biogenesis system) homologues from plant chloroplasts have been found to contain BolA-like domains, providing additional functional links.[39] Moreover, a recent proteomics investigation identified GrxD as being capable of forming a disulfide bond with the active site cysteine of *E. coli* SufE.[40] A body of evidence therefore now links GrxD, and by extension BolA, to bacterial FeS cluster biosynthesis and suggests that GrxD forms both a homodimeric complex and a heterodimeric complex with BolA. This arrangement bears some similarity to that of Grx3/4p and Fra2p in *S. cerevisiae*; however, in *E. coli* the situation is complicated by the lack of cellular compartmentalization which permits GrxD (and BolA) free access to the Isc or Suf FeS cluster biosynthesis apparatuses.

A GrxD-BolA Heterodimer Displays Increased Stability over a GrxD Homodimeric Complex. We sought to

dx.doi.org/10.1021/bi2008883 | *Biochemistry* 2011, 50, 8957–8969

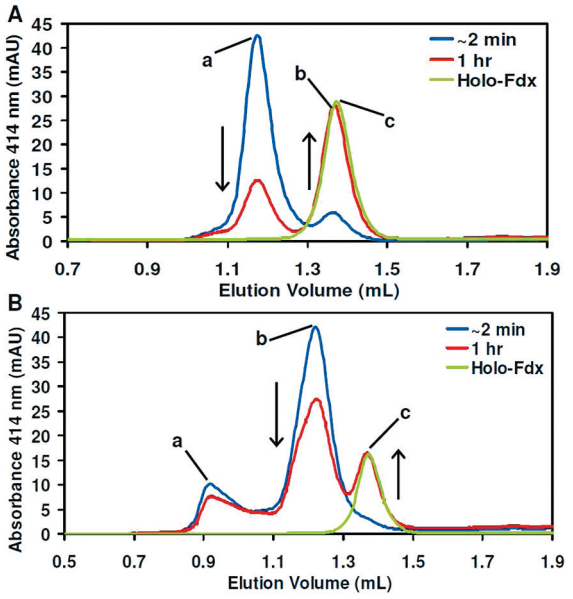

Figure 7. Analytical gel filtration analysis of the transfer of an FeS cluster from GrxD homodimer or GrxD-BolA heterodimer to apo-Fdx. (A) FeS transfer from GrxD. Average apparent MW: (a) GrxD homodimer = 39.4 ± 1.3 kDa; (b) Holo-Fdx (from transfer) = 16.6 ± 0.1 kDa; and (c) Holo-Fdx (as prepared and reconstituted) = 16.2 ± 0 kDa. Expected MW: GrxD homodimer = 30 084 Da; GrxD monomer = 15 042 Da; and Fdx = 13 598 Da. As prepared Fdx was used as the "Holo-Fdx" control sample which was run in a separate experiment. Consistent with GrxD, Fdx also migrates slightly larger than its expected MW, possibly due to an atypical nonglobular structure. Holo-Fdx profile was normalized to the 1 h profile (timed profiles at ~2 min and 1 h were not normalized). (B) FeS transfer from GrxD-BolA. Average apparent MW: (a) tetramer of GrxD-BolA heterodimer = 120 ± 10.8 kDa; (b) GrxD-BolA heterodimer = 30.6 ± 0.3 kDa; and (c) Holo-Fdx (as prepared and reconstituted) = 16.2 ± 0 kDa. Expected MW: GrxD-BolA heterodimer = 27 317 Da. All profiles were baseline corrected.

characterize the complexes formed by GrxD and/or BolA in *E. coli* and attempt to functionally decouple the role that each of these complexes play in FeS cluster biosynthesis. While the heterodimer can exist in both the cluster free and cluster bound forms (Figure 4), GrxD homodimer formation was not observed without the binding of an FeS cluster. The slightly higher MW of the holo heterodimer in comparison to its apo form (Table 1) may be accounted for by the additional mass of the bound FeS cluster, which consists of two iron atoms, two sulfur atoms, and one (possibly two) glutathione molecule(s). Thus, it appears that heterodimeric GrxD complexes display increased stability over their homodimeric counterparts, which was also observed in yeast.[14] The incubation of increasing equivalents of BolA with reconstituted holo-GrxD resulted in the almost complete conversion of the CD spectrum from the homodimeric to heterodimeric spectrum. Therefore, in a competitive environment, BolA can (apparently) displace a GrxD protomer to form a GrxD-BolA FeS containing heterodimer, further highlighting the greater relative affinity and stability of the *E. coli* heterodimer over the homodimer complex (Figure 5B).

Intact FeS Cluster Transfer from GrxD Homodimeric and Heterodimeric Complexes. The significant distinctions in the stability and physical properties (Figures S8 and S9) of the GrxD homodimer and GrxD-BolA heterodimer provided impetus for studying whether these physical variations translated into functional differences that could be relevant to FeS cluster biosynthesis. The chloroplast mono-Grx, GrxS14, was shown to rapidly and quantitatively transfer its FeS cluster to apo chloroplast Fdx *in vitro*,[24] with transfer occurring even faster than the previously reported HscA/HscB/ATP-mediated FeS cluster transfer from an IscU scaffold protein to apo-IscFdx.[41] Hence, we investigated the ability of the GrxD homodimer and GrxD-BolA heterodimer to donate their FeS clusters to a model apoprotein, which could indicate a role for them as a putative scaffold or carrier protein in FeS cluster assembly. Although both complexes are able to transfer their FeS clusters to apo-Fdx, our results demonstrate that the GrxD homodimer is a better FeS cluster donor than the GrxD-BolA heterodimer (Figure 6C, Figure 7A,B, and Figure S11). FeS cluster transfer from chloroplast mono-Grx was evaluated to be 60% complete after 5 min and 100% complete after 1 h.[24] With respect to the *E. coli* GrxD homodimer, we estimate that FeS cluster transfer is ~10% complete after ~2 min and ~75% complete after 1 h (Figure 7A). Therefore, we believe that the GrxD homodimer is an efficient scaffold protein since FeS cluster donation from GrxD occurs at approximately the same order of magnitude as chloroplast mono-Grx, the most efficient scaffold protein reported thus far.

Recent work published on the X-ray crystal structure of dimeric [2Fe−2S] containing *E. coli* holo-GrxD may shed some light on the mechanism by which GrxD can transfer its FeS cluster.[19] A comparison of the monomeric and dimeric GrxD structures has revealed subtle but functionally significant variations. For example, Lys-22 and Cys-30, which bind glutathione and iron, respectively, are not in a position to make these contacts in the monomeric conformation.[18,19] It has been suggested that the switch of GrxD from a dimeric to monomeric state is coupled to the obligate release of the FeS cluster, representing a means by which GrxD can promote FeS cluster transfer. The factors or signals which promote this conformational change are not known; however, our identification of BolA as forming a complex with GrxD suggests that BolA may be a factor which regulates this conformational switch. Both *E. coli* BolA and GrxD are expressed in the stationary phase.[17,42] One can speculate that increased expression and high cellular levels of BolA could promote the conversion of a GrxD homodimer into a GrxD-BolA heterodimer complex as observed *in vitro* (Figure 5B). This transition could represent a mechanism by which BolA limits the cellular activity of the GrxD homodimer, resulting in a concomitant increase in the activity of the GrxD-BolA heterodimeric complex.

Potential Functional Roles for Homodimeric and Heterodimeric GrxD Containing Complexes. An alternative role for mono-Grx homodimers in intracellular iron trafficking and sensing has been proposed based on recent work in yeast. Specifically, Grx3/4p have been suggested to play a role in the donation of iron for the formation of iron bound cofactors. Interestingly, despite sufficient iron levels in the cytosol, iron-dependent reactions were impaired in *grx3/grx4* mutants, suggesting that iron was not being delivered to proteins or mitochondria.[16] The lack of key iron dependent enzymes, and not oxidative stress as caused by increased cellular iron levels, has been highlighted as the major cause of severe growth defects in these strains. In contrast, the *grxD* mutant displays no growth defect on rich medium (data not shown) and exhibits sensitivity to 2′,2-dipyridyl (Figure 1). While these

data suggest that the *grxD* mutant is deficient in an iron-dependent process at low iron concentrations (consistent with a potential role as an iron donor), the lack of a severe growth defect on rich medium argues against GrxD being a generic iron chaperone/donor. Experiments are ongoing to evaluate the possible roles of GrxD in both *in vivo* iron donation and intact cluster transfer to candidate iron-dependent and FeS cluster-dependent enzymes.

Our observation that the GrxD-BolA heterodimer was not as efficient as the homodimer at mediating FeS cluster transfer to a generic apo acceptor protein such as apo-Fdx suggests that the heterodimer has little potential for being a generic FeS cluster scaffold or carrier protein. This reasoning is further supported by analytical gel filtration data which demonstrates that in contrast to the GrxD homodimer, where dimer formation was not observed without the binding of an FeS cluster, the heterodimer complex was stable even in the absence of a bound FeS cluster at higher concentrations (Figure 4A). Conversion of holo-GrxD from the dimeric to monomeric form and release of the cluster appear to be intimately coupled and likely triggered by the presence of an apo acceptor protein (data not shown).[10,19] Therefore, if an analogous mechanism is responsible for intact cluster release from the heterodimer, then the greater stability of the heterodimer (and a further increase in stability in the holo form) would inhibit FeS cluster transfer, making the heterodimer complex a poor candidate as a generic FeS cluster scaffold or carrier. These observations do not however rule out the possibility that the GrxD-BolA heterodimer may instead act as an FeS cluster scaffold/carrier for a very specific protein partner. Finally, we cannot exclude a role for *E. coli* GrxD-BolA in the regulation of sulfur and/or FeS cluster flux through or regulation of the Suf system itself as suggested by Bandyopadhyay et al.[24] Evidence comes from the observation of synthetically sick or lethal phenotypes in genetic interaction studies of *grxD* and *isc* double mutants and observation of a disulfide link between GrxD and the active site cysteine of a SufE sulfur transfer protein,[40] homologues of which in plant chloroplasts have been shown to contain BolA-like domains. We are currently investigating the interactions of GrxD and BolA with Suf components.

While homologous GrxD and BolA complexes have been characterized in yeast, we describe here the first characterization of such a complex in a prokaryote and, more importantly, the first report of intact FeS cluster transfer from a GrxD-BolA complex to an apo acceptor protein in any species. Moreover, we have shown that the *E. coli* GrxD homodimeric complex displays markedly more efficient cluster transfer when compared to the GrxD-BolA heterodimer, which correlates with their overall stability, and indicates that these complexes likely perform different functional roles associated with FeS cluster biosynthesis. Further detailed analysis of the role of each of these complexes, the pathways in which they function, and any potential functional redundancy is required to understand the molecular basis of *grxD* synthetic lethal interactions with the Isc FeS cluster biosynthesis system.

■ ASSOCIATED CONTENT

Supporting Information

Summary of bacterial strains and plasmids used in this work (Table S1); MS of as prepared GrxD (Figure S1), analytical gel filtration elution profile of apo-GrxD monomer (Figure S2), SDS-PAGE analysis of GrxD (Figure S3), CD spectroscopy of GrxD (Figure S4), MS of reconstituted GrxD homodimer (Figure S5), concentration-dependent analytical gel filtration profile of BolA (Figure S6), MS of BolA (Figure S7), analytical gel filtration elution profiles of reconstituted GrxD homodimer and reconstituted GrxD-BolA heterodimer (Figure S8), UV−vis of reconstituted GrxD homodimer and reconstituted GrxD-BolA heterodimer (Figure S9), MS of GrxD-BolA heterodimer (Figure S10), FeS cluster transfer from GrxD-BolA heterodimer to apo-Fdx (Figure S11). This material is available free of charge via the Internet at http://pubs.acs.org.

■ AUTHOR INFORMATION

Corresponding Author

*E-mail: gpbutland@lbl.gov. Tel: 510-486-6905. Fax: 510-495-2723.

Funding

This work was supported by Award GM088196 from the National Institute of General Medical Sciences. This work was also supported by the Director, Office of Science, of the U.S. Department of Energy under Contract DE-AC02-05CH11231 through an award to G.B. and an E. O. Lawrence Fellowship to N.Y., the National Science Foundation (CHE-1012833 to E.R.W.), and an NIH training grant (T32GM08295) to H.J.S. The content is solely the responsibility of the authors and does not necessarily represent the official views of the National Institute of General Medical Sciences or the National Institutes of Health.

■ ACKNOWLEDGMENTS

We acknowledge S. Allen, E. D. Szakal, and H. E. Witkowska for MS protein identification that was performed at the UCSF Sandler-Moore Mass Spectrometry Core Facility, supported in part by the Sandler Family Foundation, the Gordon and Betty Moore Foundation, and NIH/NCI Cancer Center Support Grant P30 CA082103. We thank A. Saini (LBNL, Berkeley) for insightful comments on the manuscript.

■ ABBREVIATIONS

mono-Grx, monothiol glutaredoxin; Trx, thioredoxin; FeS, iron−sulfur; Isc, iron−sulfur cluster; Suf, sulfur utilization factor; Fdx, ferredoxin; ESI, electrospray ionization; MS, mass spectrometry; LC, liquid chromatography; MALDI, matrix-assisted laser desorption/ionization; DTT, dithiothreitol; SPA, sequential peptide affinity; CD, circular dichroism; BCA, bicinchoninic acid; EDTA, ethylenediaminetetraacetic acid; MW, molecular weight; Met, methionine.

■ REFERENCES

(1) Herrero, E., and de la Torre-Ruiz, M. A. (2007) Monothiol glutaredoxins: a common domain for multiple functions. *Cell. Mol. Life Sci. 64*, 1518−1530.

(2) Witte, S., Villalba, M., Bi, K., Liu, Y. H., Isakov, N., and Altman, A. (2000) Inhibition of the c-Jun N-terminal kinase/AP-1 and NF-kappa B pathways by PICOT, a novel protein kinase C-interacting protein with a thioredoxin homology domain. *J. Biol. Chem. 275*, 1902−1909.

(3) Babichev, Y., and Isakov, N. (2001) Tyrosine phosphorylation of PICOT and its translocation to the nucleus in response of human T cells to oxidative stress. *Adv. Exp. Med. Biol. 495*, 41−45.

(4) Kato, N., Motohashi, S., Okada, T., Ozawa, T., and Mashima, K. (2008) PICOT, protein kinase C theta-interacting protein, is a novel regulator of Fc epsilon RI-mediated mast cell activation. *Cell. Immunol. 251*, 62−67.

(5) Rouhier, N., Couturier, J., Johnson, M. K., and Jacquot, J. P. (2010) Glutaredoxins: roles in iron homeostasis. *Trends Biochem. Sci. 35*, 43−52.
(6) Muhlenhoff, U., Gerber, J., Richhardt, N., and Lill, R. (2003) Components involved in assembly and dislocation of iron-sulfur clusters on the scaffold protein Isu1p. *EMBO J. 22*, 4815−4825.
(7) Ojeda, L., Keller, G., Muhlenhoff, U., Rutherford, J. C., Lill, R., and Winge, D. R. (2006) Role of glutaredoxin-3 and glutaredoxin-4 in the iron regulation of the Aft1 transcriptional activator in *Saccharomyces cerevisiae*. *J. Biol. Chem. 281*, 17661−17669.
(8) Pujol-Carrion, N., Belli, G., Herrero, E., Nogues, A., and de la Torre-Ruiz, M. A. (2006) Glutaredoxins Grx3 and Grx4 regulate nuclear localisation of Aft1 and the oxidative stress response in *Saccharomyces cerevisiae*. *J. Cell Sci. 119*, 4554−4564.
(9) Molina, M. M., Belli, G., de la Torre, M. A., Rodriguez-Manzaneque, M. T., and Herrero, E. (2004) Nuclear monothiol glutaredoxins of *Saccharomyces cerevisiae* can function as mitochondrial glutaredoxins. *J. Biol. Chem. 279*, 51923−51930.
(10) Picciocchi, A., Saguez, C., Boussac, A., Cassier-Chauvat, C., and Chauvat, F. (2007) CGFS-type monothiol glutaredoxins from the cyanobacterium *Synechocystis* PCC6803 and other evolutionary distant model organisms possess a glutathione-ligated [2Fe-2S] cluster. *Biochemistry 46*, 15018−15026.
(11) Molina-Navarro, M. M., Casas, C., Piedrafita, L., Belli, G., and Herrero, E. (2006) Prokaryotic and eukaryotic monothiol glutaredoxins are able to perform the functions of Grx5 in the biogenesis of Fe/S clusters in yeast mitochondria. *FEBS Lett. 580*, 2273−2280.
(12) Krogan, N. J., Cagney, G., Yu, H., Zhong, G., Guo, X., Ignatchenko, A., Li, J., Pu, S., Datta, N., Tikuisis, A. P., Punna, T., Peregrin-Alvarez, J. M., Shales, M., Zhang, X., Davey, M., Robinson, M. D., Paccanaro, A., Bray, J. E., Sheung, A., Beattie, B., Richards, D. P., Canadien, V., Lalev, A., Mena, F., Wong, P., Starostine, A., Canete, M. M., Vlasblom, J., Wu, S., Orsi, C., Collins, S. R., Chandran, S., Haw, R., Rilstone, J. J., Gandi, K., Thompson, N. J., Musso, G., Onge, P. St, Ghanny, S., Lam, M. H., Butland, G., Altaf-Ul, A. M., Kanaya, S., Shilatifard, A., O'Shea, E., Weissman, J. S., Ingles, C. J., Hughes, T. R., Parkinson, J., Gerstein, M., Wodak, S. J., Emili, A., and Greenblatt, J. F. (2006) Global landscape of protein complexes in the yeast *Saccharomyces cerevisiae*. *Nature 440*, 637−643.
(13) Kumanovics, A., Chen, O. S., Li, L., Bagley, D., Adkins, E. M., Lin, H., Dingra, N. N., Outten, C. E., Keller, G., Winge, D., Ward, D. M., and Kaplan, J. (2008) Identification of FRA1 and FRA2 as genes involved in regulating the yeast iron regulon in response to decreased mitochondrial iron-sulfur cluster synthesis. *J. Biol. Chem. 283*, 10276−10286.
(14) Li, H., Mapolelo, D. T., Dingra, N. N., Naik, S. G., Lees, N. S., Hoffman, B. M., Riggs-Gelasco, P. J., Huynh, B. H., Johnson, M. K., and Outten, C. E. (2009) The yeast iron regulatory proteins Grx3/4 and Fra2 form heterodimeric complexes containing a [2Fe-2S] cluster with cysteinyl and histidyl ligation. *Biochemistry 48*, 9569−9581.
(15) Li, H., Mapolelo, D. T., Dingra, N. N., Keller, G., Riggs-Gelasco, P., Winge, D. R., Johnson, M. K., and Outten, C. E. (2011) Histidine-103 in Fra2 is an iron-sulfur cluster ligand in the [2Fe-2S] Fra2-Grx3 complex and is required for in vivo iorn signaling in yeast. *J. Biol. Chem. 286*, 867−876.
(16) Muhlenhoff, U., Molik, S., Godoy, J. R., Uzarska, M. A., Richter, N., Seubert, A., Zhang, Y., Stubbe, J., Pierrel, F., Herrero, E., Lillig, C. H., and Lill, R. (2010) Cytosolic monothiol glutaredoxins function in intracellular iron sensing and trafficking via their bound iron-sulfur cluster. *Cell Metab. 12*, 373−385.
(17) Fernandes, A. P., Fladvad, M., Berndt, C., Andresen, C., Lillig, C. H., Neubauer, P., Sunnerhagen, M., Holmgren, A., and Vlamis-Gardikas, A. (2005) A novel monothiol glutaredoxin (Grx4) from *Escherichia coli* can serve as a substrate for thioredoxin reductase. *J. Biol. Chem. 280*, 24544−24552.
(18) Fladvad, M., Bellanda, M., Fernandes, A. P., Mammi, S., Vlamis-Gardikas, A., Holmgren, A., and Sunnerhagen, M. (2005) Molecular mapping of functionalities in the solution structure of reduced Grx4, a monothiol glutaredoxin from *Escherichia coli*. *J. Biol. Chem. 280*, 24553−24561.
(19) Iwema, T., Picciocchi, A., Traore, D. A., Ferrer, J. L., Chauvat, F., and Jacquamet, L. (2009) Structural basis for delivery of the intact [Fe2S2] cluster by monothiol glutaredoxin. *Biochemistry 48*, 6041−6043.
(20) Tokumoto, U., and Takahashi, Y. (2001) Genetic analysis of the isc operon in *Escherichia coli* involved in the biogenesis of cellular iron-sulfur proteins. *J. Biochem. 130*, 63−71.
(21) Takahashi, Y., and Tokumoto, U. (2002) A third bacterial system for the assembly of iron-sulfur clusters with homologs in archaea and plastids. *J. Biol. Chem. 277*, 28380−28383.
(22) Outten, F. W., Djaman, O., and Storz, G. (2004) A suf operon requirement for Fe-S cluster assembly during iron starvation in *Escherichia coli*. *Mol. Microbiol. 52*, 861−872.
(23) Butland, G., Babu, M., Diaz-Mejia, J. J., Bohdana, F., Phanse, S., Gold, B., Yang, W., Li, J., Gagarinova, A. G., Pogoutse, O., Mori, H., Wanner, B. L., Lo, H., Wasniewski, J., Christopolous, C., Ali, M., Venn, P., Safavi-Naini, A., Sourour, N., Caron, S., Choi, J. Y., Laigle, L., Nazarians-Armavil, A., Deshpande, A., Joe, S., Datsenko, K. A., Yamamoto, N., Andrews, B. J., Boone, C., Ding, H., Sheikh, B., Moreno-Hagelseib, G., Greenblatt, J. F., and Emili, A. (2008) eSGA: *E. coli* synthetic genetic array analysis. *Nature Methods 5*, 789−795.
(24) Bandyopadhyay, S., Gama, F., Molina-Navarro, M. M., Gualberto, J. M., Claxton, R., Naik, S. G., Huynh, B. H., Herrero, E., Jacquot, J. P., Johnson, M. K., and Rouhier, N. (2008) Chloroplast monothiol glutaredoxins as scaffold proteins for the assembly and delivery of [2Fe-2S] clusters. *EMBO J. 27*, 1122−1133.
(25) Huynen, M. A., Spronk, C. A., Gabaldon, T., and Snel, B. (2005) Combining data from genomes, Y2H and 3D structure indicates that BolA is a reductase interacting with a glutaredoxin. *FEBS Lett. 579*, 591−596.
(26) von Mering, C., Huynen, M., Jaeggi, D., Schmidt, S., Bork, P., and Snel, B. (2003) STRING: a database of predicted functional associations between proteins. *Nucleic Acids Res. 31*, 258−261.
(27) Aldea, M., Garrido, T., Hernandez-Chico, C., Vicente, M., and Kushner, S. R. (1989) Induction of a growth-phase-dependent promoter triggers transcription of bolA, an *Escherichia coli* morphogene. *EMBO J. 8*, 3923−3931.
(28) Santos, J. M., Lobo, M., Matos, A. P., De Pedro, M. A., and Arraiano, C. M. (2002) The gene bolA regulates dacA (PBP5), dacC (PBP6) and ampC (AmpC), promoting normal morphology in *Escherichia coli*. *Mol. Microbiol. 45*, 1729−1740.
(29) Vieira, H. L., Freire, P., and Arraiano, C. M. (2004) Effect of *Escherichia coli* morphogene bolA on biofilms. *Appl. Environ. Microbiol. 70*, 5682−5684.
(30) Freire, P., Vieira, H. L., Furtado, A. R., de Pedro, M. A., and Arraiano, C. M. (2006) Effect of the morphogene bolA on the permeability of the *Escherichia coli* outer membrane. *FEMS Microbiol. Lett. 260*, 106−111.
(31) Butland, G., Peregrin-Alvarez, J. M., Li, J., Yang, W., Yang, X., Canadien, V., Starostine, A., Richards, D., Beattie, B., Krogan, N., Davey, M., Parkinson, J., Greenblatt, J., and Emili, A. (2005) Interaction network containing conserved and essential protein complexes in *Escherichia coli*. *Nature 433*, 531−537.
(32) Nakamura, M., Saeki, K., and Takahashi, Y. (1999) Hyperproduction of recombinant ferredoxins in *Escherichia coli* by coexpression of the ORF1-ORF2-iscS-iscU-iscA-hscB-hs cA-fdx-ORF3 gene cluster. *J. Biochem. 126*, 10−18.
(33) Tokumoto, U., Nomura, S., Minami, Y., Mihara, H., Kato, S., Kurihara, T., Esaki, N., Kanazawa, H., Matsubara, H., and Takahashi, Y. (2002) Network of protein-protein interactions among iron-sulfur cluster assembly proteins in *Escherichia coli*. *J. Biochem. 131*, 713−719.
(34) Guzman, L. M., Belin, D., Carson, M. J., and Beckwith, J. (1995) Tight regulation, modulation, and high-level expression by vectors containing the arabinose PBAD promoter. *J. Bacteriol. 177*, 4121−4130.
(35) Baba, T., Ara, T., Hasegawa, M., Takai, Y., Okumura, Y., Baba, M., Datsenko, K. A., Tomita, M., Wanner, B. L., and Mori, H. (2006)

Construction of *Escherichia coli* K-12 in-frame, single-gene knockout mutants: the Keio collection. *Mol. Syst. Biol. 2*, 0008.

(36) Nishio, K., and Nakai, M. (2000) Transfer of iron-sulfur cluster from NifU to apoferredoxin. *J. Biol. Chem. 275*, 22615−22618.

(37) Angelini, S., Gerez, C., Ollagnier-de Choudens, S., Sanakis, Y., Fontecave, M., Barras, F., and Py, B. (2008) NfuA, a new factor required for maturing Fe/S proteins in *Escherichia coli* under oxidative stress and iron starvation conditions. *J. Biol. Chem. 283*, 14084−14091.

(38) Hoffmann, B., Uzarska, M. A., Berndt, C., Godoy, J. R., Haunhorst, P., C., H. L., Lill, R., and Muhlenhoff, U. (2011) The multi-domain thioredoxin-monothiol glutaredoxins represent a distinct functional group. *Antioxid. Redox Sign. 15*, 19−30.

(39) Ye, H., Abdel-Ghany, S. E., Anderson, T. D., Pilon-Smits, E. A. H., and Pilon, M. (2006) CpSufE activates the cysteine desulfurase CpNifS for chloroplastic Fe-S cluster formation. *J. Biol. Chem. 281*, 8958−8969.

(40) Bolstad, H. M., and Wood, M. J. (2010) An in vivo method for characterization of protein interactions within sulfur trafficking systems of *E. coli*. *J. Proteome Res. 9*, 6740−6751.

(41) Chandramouli, K., and Johnson, M. K. (2006) HscA and HscB stimulate [2Fe-2S] cluster transfer from IscU to apoferredoxin in an ATP-dependent reaction. *Biochemistry 45*, 11087−11095.

(42) Lange, R., and Henggearonis, R. (1991) Growth phase-regulated expresssion of bolA and morphology of stationary-phase *Escherichia coli* cells are controlled by the novel sigma factor sigma S. *J. Bacteriol. 173*, 4474−4481.